

Pediatric Chest MDCT Using Tube Current Modulation: Effect on Radiation Dose with Breast Shielding

Courtney Coursey¹
 Donald P. Frush¹
 Terry Yoshizumi²
 Greta Toncheva²
 Giao Nguyen²
 S. Bruce Greenberg³

Keywords: CT, CT technology, MDCT, pediatric chest CT, phantoms, radiation dose reduction, shielding

DOI:10.2214/AJR.07.2017

The bismuth material for this study was provided by F & L Medical Products.

D. P. Frush receives unrestricted research support from GE Healthcare.

Received February 6, 2007; accepted after revision July 22, 2007.

¹Division of Pediatric Radiology, Department of Radiology, Box 3808, Duke University Medical Center, Durham, NC 27710. Address correspondence to D. P. Frush (frush943@mc.duke.edu).

²Radiation Safety Division, Duke University Medical Center, Durham, NC.

³Department of Radiology, University of Arkansas for Medical Sciences and Arkansas Children's Hospital, Little Rock, AR.

CME

This article is available for CME credit. See www.arrs.org for more information.

WEB

This is a Web exclusive article.

AJR 2008; 190:W54–W61

0361–803X/08/1901–W54

© American Roentgen Ray Society

OBJECTIVE. The purpose of our study was to assess the effect on radiation dose and image noise during pediatric chest 16-MDCT using automatic tube current modulation and bismuth breast shields.

MATERIALS AND METHODS. Age-based chest 16-MDCT was performed on an anthropomorphic phantom representing a 5-year-old child. Two scans were obtained in each of four sequences: first, without a shield; second, with a 2-ply bismuth shield; third, using automatic tube current modulation with a scout image obtained after placement of the shield; and fourth, using automatic tube current modulation with a scout image obtained before placement of the shield. Metal oxide semiconductor field effect transistor technology was used to measure the radiation dose in 20 organ locations. Effective dose was estimated using the console dose–length product. Noise was measured by recording the SD of Hounsfield units in identical regions of interest.

RESULTS. The bismuth breast shield reduced the dose to the breast by 26%. Shielding and automatic tube current modulation reduced the breast dose by 52%. Multiple organ doses were lowest when the shield was placed after the scout radiograph had been obtained. When the shield was placed after the scout image was obtained, the mean noise in the range of shielding increased from 11.4 to 13.1 H (superior mediastinum) and from 10.0 to 12.8 H (heart) ($p < 0.01$). Increased noise, however, was near the target noise index (measured in SD of Hounsfield units) of 12.0 H (SD). Using automatic tube current modulation, the effective dose was reduced by 35% when the shield was placed after the scout and by 20% when the shield was present in the scout.

CONCLUSION. The greatest dose reduction is achieved by placing the shield after obtaining the scout image to avoid Auto mA compensation due to density of shield. With this technique, image noise increased but remained close to the target noise index.

An estimated 57 million CT examinations were performed in the United States in 2000 [1]. It is also estimated that approximately 7.1 million CT examinations were performed in pediatric patients in 2002 [2]. Because of the large number of examinations and the relatively high radiation dose delivered by CT, techniques should minimize the radiation dose to the patient while still providing diagnostic quality—the ALARA (as low as reasonably achievable) principle. Radiation dose is of special concern for the pediatric patient population because the younger the child at exposure, the greater the potential for cancer development [3, 4].

Two techniques that have independently been shown to lower CT radiation dose are automatic tube current modulation [5–12]

and bismuth shielding [13–15]. Automatic tube current modulation using both angular (x,y -axis) and longitudinal (z -axis) techniques has been shown to reduce patient dose [5–12]. Shielding has also been shown to reduce radiation dose, primarily from attenuation of the primary beam.

The combined use of automatic tube current modulation and a shielding device might be expected to reduce radiation dose more than either technique alone. However, it may also be that automatic tube current modulation technology that modulates in the z -axis on the basis of the topogram (scout image) may compensate for the presence of the shield by increasing the tube current and thus increasing the dose during the diagnostic scan when the shield is present while the scout image is obtained. To our knowledge,

Pediatric Chest MDCT with Tube Current Modulation

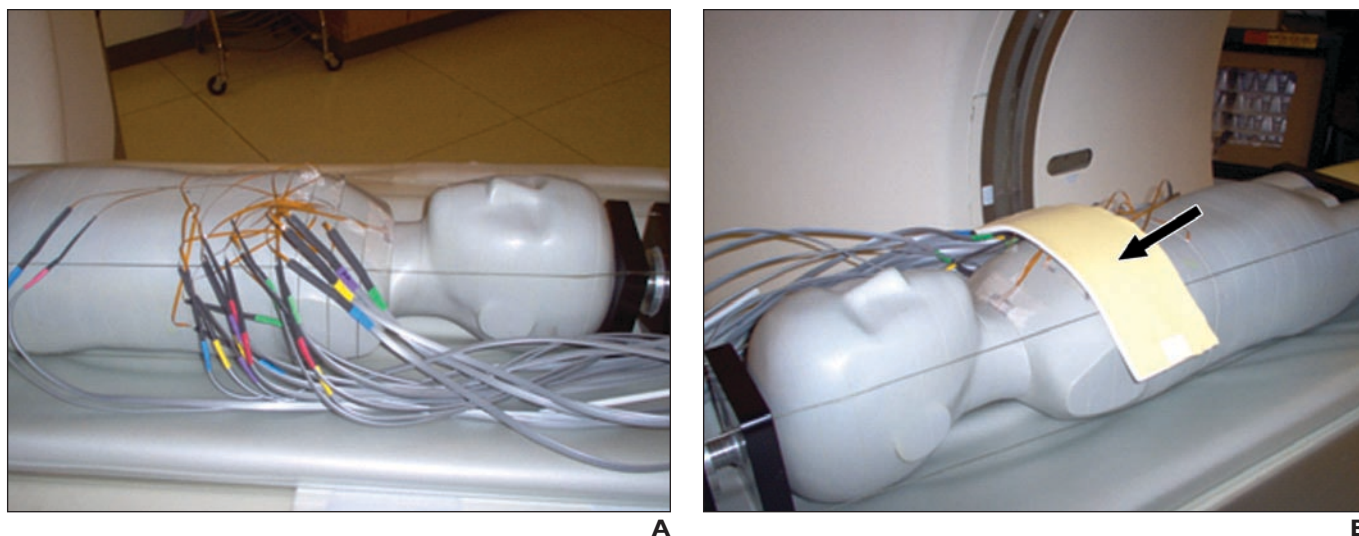


Fig. 1—Phantom and shield used in this study.

A, Anthropomorphic phantom representing 5-year-old child (Atom Pediatric 5-Year-Old Phantom, model 705-D CIRS) with metal oxide semiconductor field effect transistor (MOSFET) (Autosense MOSFET system, Best Medical Canada) detectors in place.

B, Bismuth (F & L Medical Products) breast shield (*arrow*) in place.

dosimetry during MDCT using the combination of bismuth shielding and automatic tube current modulation has not been reported. Therefore, the purpose of our study was to determine the effect on radiation dose and to measure image quality (noise) of images obtained using bismuth breast shields with z-axis automatic tube current modulation during pediatric chest MDCT.

Materials and Methods

An anthropomorphic phantom representing a 5-year-old child (Atom Pediatric 5-Year-Old Phantom, model 705-D, CIRS) was used (Fig. 1). The specific dimensions of the phantom are weight, 19 kg; height, 110 cm; thorax dimensions, 14 × 17 cm. This phantom was scanned using the technique clinically used for the 5-year-old age-based chest CT protocol (16-MDCT, LightSpeed, GE Healthcare) consisting of 120 kVp, 0.5-second rotation time, 1.375 pitch, 16 × 1.25 mm effective collimation, 5-mm slice thickness, 2.5-mm reconstruction interval, and a small scanning field of view, with images reconstructed in a standard algorithm. The phantom was first scanned with a fixed tube current of 65 mA without a breast shield. The phantom was next scanned using the same parameters but with the addition of a 2-ply bismuth (1.7 g/cm²) (F & L Medical Products) breast shield with a 1-cm-thick foam stand-off pad. The shield measured 9 cm in the craniocaudal dimension and was designed to cover the chest to the midaxillary line (Fig. 1). The phantom was then scanned using z-axis automatic tube current modulation (Auto mA, GE Healthcare) with 65

TABLE I: Organ Doses Using MOSFET During Chest MDCT in Phantom Representing a 5-Year-Old Child

Organ	Slice, Location ^b	Dose (cGy) ^a			
		Without Shield or ATCM	With Shield, Without ATCM	Scout With Shield, With ATCM	Scout Without Shield, With ATCM
Breast (l)	12, 58	0.40	0.31	0.17	0.17
Breast (r)	12, 59	0.35	0.25	0.19	0.19
Skin above breast	12, –	0.37	0.28	0.20	0.20
Skin above sternum	12, –	0.48	0.32	0.29	0.18
Esophagus and heart	12, 51	0.36	0.34	0.26	0.19
Bone marrow, sternum	11, 39	0.31	0.29	0.20	0.12
Bone marrow, ribs (l)	11, 40	0.30	0.24	0.19	0.13
Bone marrow, ribs (r)	11, 45	0.38	0.32	0.13	0.18
Bone marrow, thoracic and lumbar spine	11, 38	0.46	0.30	0.23	0.21
Lung (l) (middle)	12, 53	0.41	0.37	0.27	0.19
Lung (r) (middle)	12, 56	0.40	0.36	0.26	0.22
Lung (l) (middle)	13, 68	0.44	0.42	0.38	0.25
Lung (r) (middle)	13, 71	0.48	0.41	0.40	0.26
Thymus	12, 60	0.43	0.37	0.28	0.23
Thyroid (l) ^c	9, 24	0.45	0.44	0.24	0.25
Thyroid (r) ^c	9, 25	0.43	0.42	0.26	0.25
Liver ^c	16, 103	0.40	0.42	0.38	0.35
Stomach ^c	16, 109	0.37	0.37	0.36	0.37
Esophagus ^c	10, 35	0.40	0.36	0.24	0.23
Kidney (l) ^c	16, 116	0.33	0.31	0.31	0.28

Note—MOSFET = metal oxide semiconductor field effect transistor. ATCM = z-axis automatic tube current modulation. Dash (–) indicates detectors placed on surface of phantom.

^aAverage of two scans was obtained for each protocol.

^bOf CIRS phantom (Atom Pediatric 5-Year-Old Phantom, model 705-D).

^cLocations not underneath breast shield.

mA maximum, 10 mA minimum, and a noise index (measured in SD of Hounsfield units) of 12.0 H (SD) (all other parameters remaining the same) with the topogram (scout) frontal and lateral ra-

diographs obtained with the bismuth breast shield in place. Auto mA selects tube currents on the basis of patient density, size, and shape, as reflected in the localizer radiograph, to maintain the target

noise level (the noise index) between maximum (ceiling) and minimum levels, which are also selected [16]. The noise index approximates noise as measured in the center of a uniform phantom

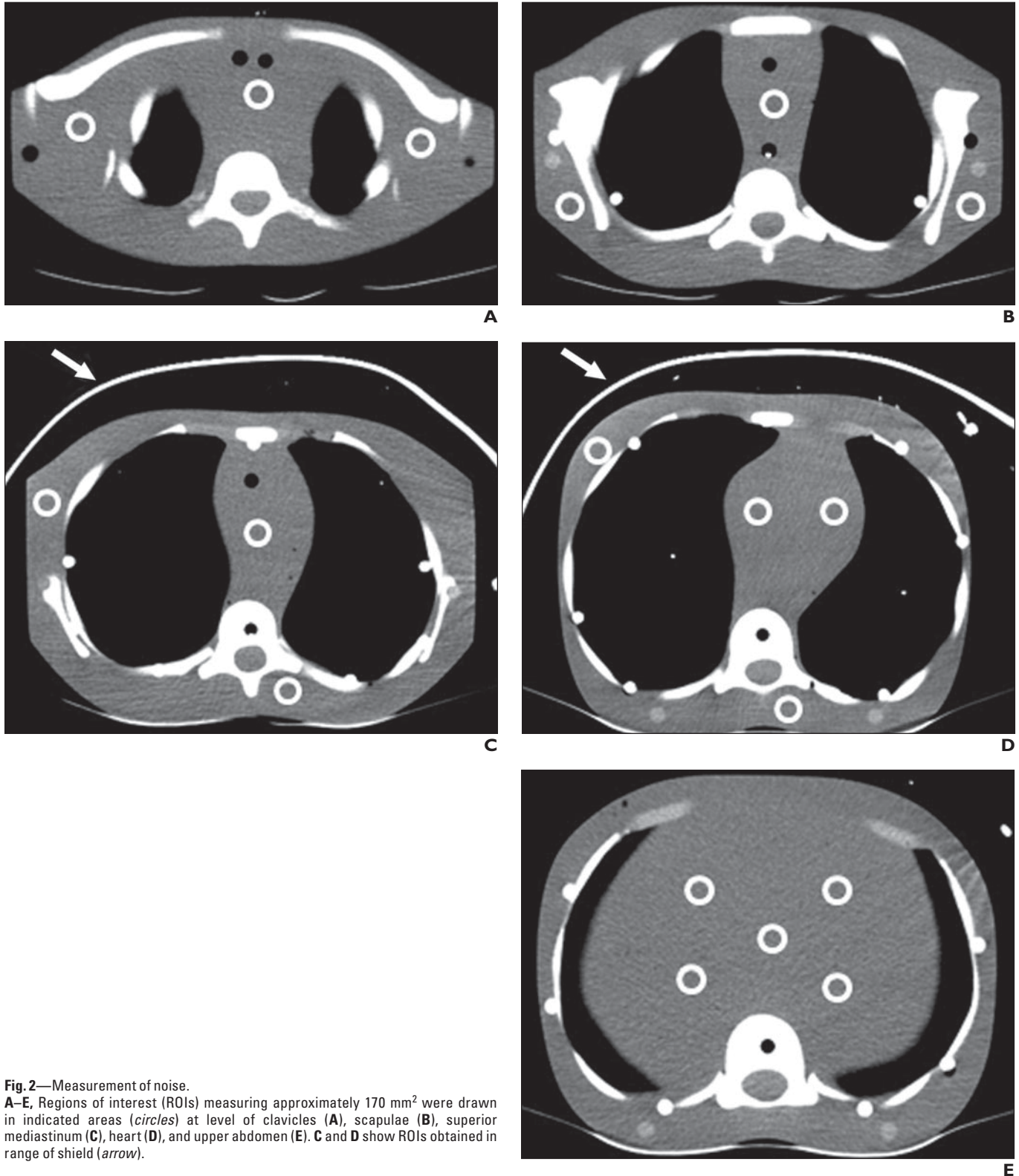


Fig. 2—Measurement of noise. **A–E,** Regions of interest (ROIs) measuring approximately 170 mm² were drawn in indicated areas (*circles*) at level of clavicles (**A**), scapulae (**B**), superior mediastinum (**C**), heart (**D**), and upper abdomen (**E**). **C** and **D** show ROIs obtained in range of shield (*arrow*).

[16]. Finally, the phantom was scanned with z-axis automatic tube current modulation using the same parameters, but the scout radiographs were obtained before the breast shield was placed.

The phantom is subdivided into 26 contiguous sections, each 25-mm thick, with assignable anatomic locations for up to 19 radiosensitive internal organs. Each section contains several 5-mm diameter through holes, with each hole location optimized for dosimetry of 19 internal organs. Each hole in the phantom is labeled with an assigned number that can be referenced to the user manual accompanying the phantom [17]. Each detector was placed in the hole at the recommended depth for these internal organs (Table 1). For skin dose, detectors were placed on the surface of the skin. The doses at 20 organ locations were measured using metal oxide semiconductor field effect transistor (MOSFET) technology (Autosense MOSFET system, Best Medical Canada; High-Sensitivity MOSFET dosimeter model TN-1002RD, Best Medical Canada). When the transistor is irradiated, the threshold voltage of the transistor shifts. This shift can be measured and is proportional to the absorbed radiation dose [18]. The calibration method for MOSFET detectors has been described in greater detail elsewhere [19, 20]. For a typical CT dose of 1 cGy (10 mGy), the percentage of uncertainty is approximately 10% or less. Scanning was performed twice for each set of imaging parameters, and the average of the two recorded doses was used for analysis. Tube current for each slice was recorded from the annotations on the images.

Dose-length product (DLP) values were recorded from the console [21] using a conversion factor of $0.021 \text{ mSv} \cdot \text{mGy}^{-1} \cdot \text{cm}^{-1}$ for 5-year-old chest MDCT. This factor was based on the fact that the adult chest conversion factor is $0.019 \text{ mSv} \cdot \text{mGy}^{-1} \times \text{cm}^{-1}$ and on previous MOSFET dosimetry determinations in our laboratory [22]. The same scanning duration was used for each manipulation.

Noise was measured as the SD of Hounsfield units by drawing regions of interest (ROIs) in homogeneous-appearing areas of the scan and recording the SD of Hounsfield units in the ROI. The size of the ROI varied depending on the region measured but was generally a 170 mm^2 circular area. Noise was measured in identical regions for each study at a total of 18 different locations in five slice levels from the soft-tissue algorithm display, as shown in Figure 2. The mean noise measurement was computed for each of the five slice levels for the four different scanning paradigms in Table 2. The relationship of these mean levels was examined using a two-way analysis of variance.

Results

The measured radiation doses detected at 20 locations using MOSFET technology are

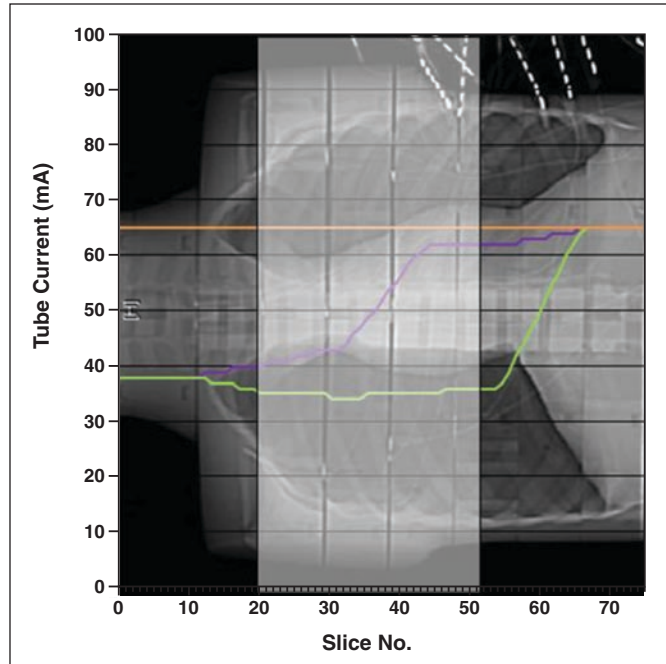


Fig. 3—Tube current generated at each slice level for each scanning paradigm: z-axis Auto mA (GE Healthcare) tube current modulation, shield present in scout image (purple); z-axis Auto mA tube current modulation, shield placed after scout image was obtained (green); fixed tube current (65 mA) scanning (orange). Slice thickness was 5 mm. White rectangle indicates location of shield.

reported in Table 1. The highest detected doses with a fixed tube current technique and no bismuth shield were in the lungs and in the skin above the sternum, where doses of 0.48 cGy were recorded. The breast doses with a fixed tube current and no bismuth shield were 0.40 cGy to the left breast and 0.35 cGy to the right breast. The lowest recorded doses with a fixed tube current and no bismuth shield were to the marrow of the left midthoracic ribs (0.30 cGy), the sternum marrow (0.31 cGy), and the left kidney (0.33 cGy) (Table 1).

With the addition of the bismuth breast shield while keeping all other scanning parameters fixed, the measured average breast dose was reduced by 26% (from 0.38 cGy to 0.28 cGy). Measured doses decreased at all 14 locations under the shield by an average of 18.0% (ranging from 5% in the left lung to 35% in the bone marrow of the spine). Compare these doses with those measured outside the shielded area where doses decreased by an average of 4% at four locations, were unchanged at one location, and increased by 5% at one location.

The changes in tube current that resulted from the different scanning paradigms are illustrated in Figure 3. A fixed tube current of 65 mA was used in the standard age-based chest protocol. By comparison, when au-

tomatic tube current modulation was used without the shield present in the scout image, the resultant tube current was lower in the lungs (34–37 mA) and increased through the upper abdomen, eventually reaching the preset tube current ceiling of 65 mA. When automatic tube current modulation was used with the shield present in the scout image, the modulation compensated for the presence of the shield by increasing tube current through the level of the shield. The tube current was 40 mA in the first section that included the shield and increased along the length of the shield, reaching 62 mA in the last section that included the shield (Fig. 3). By comparison, in the examination with automatic tube current modulation but with the scout image obtained before placement of the shield, the tube current was 36 mA in the first section that included the shield and did not increase to more than 36 mA over the entire length of the shield.

With the implementation of tube current modulation with the shield placed after the scout image was obtained, measured doses decreased (average dose decrease, 37.5%) at 19 of the 20 (95%) locations when compared with the fixed tube current scan with the breast shield (Table 1). In the remaining location, the measured dose in the stomach was unchanged (Table 1).

TABLE 2: Comparison of Mean Noise Values for Pediatric Chest MDCT

Location	Noise			Noise		
	Fixed Tube Current, Age-Based Chest CT, No Breast Shield	Fixed Tube Current, Age-Based Chest CT with Breast Shield	<i>p</i>	ATCM, Shield, Shield Present In Scout	ATCM, Shield, Shield Placed After Scout Obtained	<i>p</i>
Clavicles	9.17 (8.02–9.98)	9.17 (7.59–11.05)	1.00	11.45 (10.95–12.06)	11.24 (9.85–12.69)	0.46
Mid scapulae	9.42 (7.65–11.31)	9.62 (7.12–12.4)	0.63	11.87 (9.05–14.38)	11.9 (9.08–14.82)	0.93
Superior mediastinum ^a	8.96 (6.80–12.24)	9.42 (8.14–10.56)	0.27	11.41 (9.79–13.58)	13.06 (11.20–16.86)	0.01
Heart ^a	8.50 (7.27–9.93)	9.96 (8.93–11.51)	0.008	10.00 (8.00–10.82)	12.82 (11.55–14.36)	0.001
Upper abdomen	11.4 (10.25–12.95)	11.12 (9.90–12.68)	0.44	11.12 (9.83–11.96)	11.38 (10.06–14.06)	0.50

Note—Numbers in parentheses are minimum–maximum SD of Hounsfield units in $\approx 170 \text{ mm}^2$ region of interest. ATCM = automatic tube current modulation.
^aLocation in range of shielding.

With the implementation of tube current modulation with the shield present in the scout image, measured doses decreased at 19 of the 20 (95%) locations (average dose decrease, 25.5%) when compared with the fixed tube current scan with the breast shield (Table 1). In the remaining location, the measured dose in the left kidney was unchanged (Table 1).

Comparing the examinations with automatic tube current modulation when the shield was placed before the scout was obtained versus when the shield was placed after, measured doses were higher (average dose increase, 48%) at 10 of 14 locations (71.4%) under the shield, unchanged at three locations (21.4%) under the shield, and lower (average dose decrease, 27.8%) at one location (7.1%) under the shield when the shield was present in the scout image (Table 1).

Comparing the overall highest-dose scan (fixed tube current, age-based chest CT protocol, no shield) with the lowest-dose scan (automatic tube current modulation and bismuth shield with shield placed after scout image was obtained), measured doses decreased by an average of 51.3% in the 16 locations under the shield, ranging from a 43.2% decrease in

the left lung to a 62.5% decrease in the skin over the sternum. Of note, breast dose decreased by 51.6% when automatic tube current modulation and the bismuth shield were used with the shield placed after the scout as compared with the fixed tube current, age-based chest CT with no shield.

Image noise was measured as described earlier (Table 2). For the CT images in range of the shield, average noise measurements (SD of Hounsfield units) were 8.7 H for the fixed tube current scan, 9.7 H for the fixed tube current scan with breast shield, 10.6 H for automatic tube current modulation and breast shield with shield present in the scout, and 12.9 H for automatic tube current modulation and breast shield with shield placed after the scout was obtained (Table 3). Superior to the shield, average noise measurements were 9.3 H for the fixed tube current scan with no shield, 9.4 H for the fixed tube current scan with the breast shield, 11.7 H for automatic tube current modulation and breast shield with shield present in the scout, and 11.5 H for automatic tube current modulation and breast shield with shield placed after the scout (Table 3). Inferior to the shield, average noise mea-

surements were 11.4 H for the fixed tube current scan with no shield, 11.1 H for the fixed tube current scan with breast shield, 11.2 H for automatic tube current modulation and breast shield with shield present in the scout, and 11.4 H for automatic tube current modulation and breast shield with shield placed after the scout (Table 3). Mean noise measurements were not significantly different with the addition of the breast shield in the fixed tube current scans, except in the heart, where the noise increased from 8.50 to 9.96 H ($p = 0.008$) (Table 2). When the shield was placed after the scout was obtained with automatic tube current modulation, the mean noise measurement at the level of the heart was significantly greater (from 10.0 to 12.8 H) than when the shield was present in the scout ($p = 0.001$). Likewise, the mean noise measurement at the level of the superior mediastinum was significantly greater as compared with the scans when the shield was present in the scout (from 11.4 to 13.1 H) ($p = 0.01$). Average noise at the level of the shield was greater than the target noise index (12.0 H [SD]) when the shield was placed after the scout because automatic tube current modulation did not compensate for the presence of the shield and generated a lower tube current (34–36 mA in the range of the shield) compared with when the shield was present in the scout (tube current of 40–62 mA in the range of the shield). This lower tube current resulted in increased noise.

Using the DLP method, the effective doses were 2.0 mSv using the fixed tube current technique with and without the breast shield, as expected because DLP is independent of the scout, unlike with automatic tube current modulation, in which the DLP will depend on the scan modulation. When automatic tube current modulation is used, the projected modulations in tube current are accounted for in the DLP. The total effective dose was 1.6 mSv using automatic tube current modu-

TABLE 3: Effective Dose and Noise Determination for Chest MDCT in Phantom Representing a 5-Year-Old Child

Scanning Paradigm	Effective Dose ^a (mSv)	Noise ^b		
		Above Shield	At Shield Level	Below Shield
Fixed tube current, age-based chest CT	2.0	9.3	8.7	11.4
Fixed tube current, age-based chest CT plus breast shield	2.0	9.4	9.7	11.1
ATCM, with shield, shield present in scout image	1.6	11.7	10.6	11.2
ATCM, with shield, shield placed after scout image obtained	1.4	11.5	12.9	11.4

Note—ATCM = automatic tube current modulation in z-axis using Auto mA (GE Healthcare).

^aBased on dose-length product.

^bSD of Hounsfield units in $\approx 170 \text{ mm}^2$ region of interest.

lation with the bismuth shield present in the scout radiograph, yielding a 20% dose reduction as compared with the fixed tube current scans (Table 3). The total effective dose was 1.4 mSv using automatic tube current modulation with the bismuth shield placed after the scout radiograph was obtained, yielding a 30% dose reduction as compared with the fixed tube current scans (Table 3).

Discussion

Managing the radiation dose during pediatric chest CT is important for two reasons. First, the potential cancer risk has been shown to increase as age at radiation exposure decreases [3, 4]. Second, radiation-sensitive tissues such as the breasts [23–26] are directly irradiated during chest CT. Strategies for reducing radiation dose for pediatric chest CT include appropriate adjustments in scanning parameters [27], in-plane breast shielding (where the shield is in range of CT) [14–15], and automatic tube current modulation [5–12].

Bismuth breast shields have been shown to reduce breast radiation dose by 29% in children [14] and by 27% to 52% in adults, depending on the thickness of the shield [15]. In line with these investigations, we found a 26% dose reduction to the breast in an anthropomorphic phantom representing a 5-year-old using a 2-ply bismuth breast shield. The 4% decrease in dose at four locations not under the shield and the 5% increase in dose at one location not under the shield when the shield is added is not unexpected in that the uncertainty of the MOSFET system is approximately 10% or less for a typical CT dose of 1 cGy.

Three general techniques for automatic tube current modulation are offered by the manufacturer of the scanner used for this investigation: *z*-axis (longitudinal) modulation, *x,y*-axis (angular) modulation, and a combination of both. With *z*-axis modulation, the method used in this study, tube current is modulated along the craniocaudal dimension of the patient. For example, in the setting of chest CT with *z*-axis modulation, a relatively lower tube current is delivered through the lungs, where there is less attenuation, while a relatively higher tube current is delivered through the upper abdomen, where there is more soft-tissue attenuation. With *x,y*-axis modulation, a relatively lower tube current is delivered through the thinner portions of the patient (generally the anteroposterior dimension), and a relatively higher tube current is delivered when there is relatively more attenuation (generally the lateral dimension).

The algorithms used for automatic tube current modulation differ depending on the manufacturer [28]. The *z*-axis modulation used in this investigation (Auto mA) requires the user to select the noise index (SD of Hounsfield units) and minimum and maximum tube current values. The range between these values is where the modulation will take place.

Automatic tube current modulation in the *z*-axis has been shown to reduce tube current–time product by 18–26% in the setting of adult chest CT, depending on the noise index [7]. Automatic tube current modulation in the *x,y*-axis has been shown to reduce mAs by 31–39% in the setting of pediatric chest CT [6] and to reduce mean effective mAs by 16.9% in the setting of adult chest CT [5].

Note, however, that tube current reductions are surrogates for the actual patient dose. The current study provides additional insight into the work of prior studies by also assessing the effect on organ doses when automatic tube current modulation is used because dosimetry was performed, rather than recording estimated dose changes based on alterations in tube current. MOSFET dosimetry offers an opportunity for more accurate dose determinations in CT [19]. The 37.5% average organ dose reduction in the current anthropomorphic phantom study with the use of Auto mA tube current modulation with the shield placed after the scout image, then, is slightly higher than previously reported mAs reductions in the setting of adult chest CT with *z*-axis automatic tube current modulation. This difference may reflect a combination of different automatic tube current modulation technologies, different noise indexes, or automatic tube current modulation when used in a phantom. The 25.5% average dose reduction with Auto mA tube current modulation with the shield present in the scout is similar to previous investigations.

The locations (stomach and left kidney) in which the measured dose did not change with Auto mA were in the upper abdomen, where tube current was the same (65 mA) in the fixed tube current and the automatic tube current modulation scans, likely because an equivalent amount of tube current was necessary to maintain the target noise level. Noise levels in the sections containing the stomach and left kidney dosimeters were similar in the automatic tube current modulation and fixed tube current scans (data not shown).

The use of breast shields in combination with automatic tube current modulation has not been previously addressed. It is conceivable that with the type of *z*-axis modulation

used in this investigation (combined *z*- and *x,y*-axis modulation was not available at the time of our study), the increased attenuation present on the scout image due to the shield (and the concomitant increase in tube current in this region) could negate the benefits of both shielding and tube current modulation. We found that Auto mA *z*-axis modulation compensated for the density of the shield if the shield was present in the scout radiograph by increasing the tube current along the *z*-axis in the range of the shield (Fig. 3). As seen in Figure 3, the tube current began to increase at the leading edge of the breast shield. The rate of rise increased dramatically after 15 slices, or approximately 7.5 cm beyond the leading edge of the shield. The reason for this unexpected delay in increasing tube current is not known. Although there is a lag before modulation begins, it is relatively short (80 milliseconds). Further analysis of the data with the manufacturer did not provide an explanation (Toth T, GE Healthcare, personal communication).

However, if the modulation began sooner in the upper thorax, we would have expected an even greater dose savings with Auto mA tube current modulation when the shield was placed after the scout. That tube current did not decrease beyond the shield before reaching the abdomen can be explained by the fact that the Auto mA tube current modulation software derives the tube current on the basis of the highest attenuating structure under the detectors at a given time. A portion of the detectors was likely always either over the shield or over the upper abdomen at the end of the scanning. However, even though Auto mA compensated for the shield when the shield was present in the scout, the selected tube currents through the positions that included the shield (40–62 mA) still were lower than the fixed tube current of 65 mA used in the fixed-tube-current, age-based scan. Therefore, some but not all of the tube current benefit was lost when the shield was present in the scout radiograph.

Furthermore, we postulated that placing the shield after the scout image was obtained would maximize dose benefits from both shielding and Auto mA tube current modulation. In fact, placing the shield after the scout was obtained resulted in radiation doses (measured using MOSFET technology) that were lower at 10 locations, unchanged at three locations (right breast, left breast, skin over breasts), and increased at one location in the range of shielding. The effective dose, as expected, decreased by 13%, from 1.6 to 1.4 mSv, when the shield

was placed after the scout radiograph with Auto mA tube current modulation.

That breast dose and skin dose superficial to the breasts did not change when the shield was placed after the scout was obtained while almost all the other organ doses in the range of the shield decreased was somewhat unexpected. One explanation is that the breast detectors were located near the leading edge of the shield, where the differences in tube current were not so great (43–50 mA when shield was present in scout image vs 34–35 mA when shield was placed after scout image was obtained). Given the spiral nature of the primary beam, it is also possible that the position of the beam (e.g., posteroanterior vs anteroposterior) relative to the breast detectors was different in the automatic tube current modulation runs with shield placed before and after the scout image was obtained. A posteroanterior beam would be more attenuated by soft tissues before it reaches the breast detectors, whereas an anteroposterior beam would be attenuated by the breast shield before reaching the detectors. This phenomenon has been reported recently with MOSFET and breast dosimetry and is a limitation of this type of surface dosimetry (unlike more central dose locations) in helical as opposed to axial MDCT [29].

It was also unexpected that the average dose in the bone marrow of the right ribs increased when the shield was placed after the scout (Table 1). As noted earlier, all other measured doses in the range of the shield decreased or were unchanged when the shield was placed after the scout with Auto mA. The measured doses at this location for each of the four Auto mA runs (two with the shield present in the scout and two with the shield placed after the scout) were 0.12, 0.14, 0.13, and 0.22 cGy. The 0.22-cGy value appears to be an outlier that may have falsely elevated the average.

Breast doses of 0.1–0.7 Gy have been shown to be associated with an increased risk of breast cancer [25, 26]. Although the breast dose in our study was low (0.4 cGy without the shield), appropriately minimizing any radiation dose, especially for breast parenchyma in young individuals, is prudent. In keeping with this ALARA principle, we found that breast dose was reduced by 26% with the breast shield alone and by 52% when using the breast shield and automatic tube current modulation in an anthropomorphic phantom representing a 5-year-old child.

When measured doses decreased, image

noise increased. The highest-dose scan (fixed tube current chest CT without shielding) was also the least noisy. The lower noise measured in the nonmodulated examination was due, we think, to tube current levels that were higher than needed (such as in the lungs). For nonmodulated examinations, it is likely that protocols have evolved to maintain a minimum noise level for diagnostic quality through intrinsically higher attenuating areas, meaning other regions will have less noise than is needed. For example, in the nonmodulated examinations, average noise measurements cranial to the shield were 9.3 and 9.4 H (SD) and caudal to the shield were 11.4 and 11.1 H (SD) in the runs with and without the breast shield, respectively (Table 3).

The lowest-dose scan (automatic tube current modulation and shield, with shield placed after the scout image was obtained) was the noisiest scan. The increase in image noise at the level of the heart and superior mediastinum (in the range of shielding) when the shield was placed after the scout was significantly ($p < 0.01$) higher compared with when the shield was present in the scout radiograph with automatic tube current modulation. It is unclear why the heart and not the superior mediastinum had a significantly higher amount of noise with nonmodulated scanning with and without the shield. This may represent a statistical error.

When the shield was placed after the scout image was obtained, the measured noise index (12.9 H [SD]) in the range of shielding was slightly higher than the selected target noise index of 12.0 H (SD). Although this increase in noise is statistically significant, it does not necessarily equate to a reduction in diagnostic quality. For example, a prior investigation (Darsie J et al., presented at the 2005 annual meeting of the Radiological Society of North America) supports a noise index of 12.9 H (SD) to be in the acceptable range for pediatric chest CT. In addition, the target noise index was 12.0 H (SD), and the breast shields increased noise above this level by 0.9 H (SD), a difference that is arguably below threshold for visual detection. In the automatic tube current modulation runs, not unexpectedly, noise measurements were similar both cranial to and caudal to the shield. The automatic tube current modulation algorithm modulates tube current to maintain a constant noise level throughout the scanning.

Limitations of our study include that only one type of CT scanner and therefore only one automatic tube current modulation tech-

nology was investigated. For example, not all automatic tube current modulation products described by McCollough et al. [28] modulate on the basis of the scout radiograph. Therefore, the effect of placing the shield before or after the scout radiograph cannot be predicted in these settings. The use of an anthropomorphic phantom representing a single age is also a limitation of this study. However, it is expected that similar dose reductions would be seen with anthropomorphic phantoms representing different ages. Also, because there are no respiratory or cardiac motion artifacts in a phantom study, the doses and image noise changes we found may not completely translate into a patient study. The use of the SD of Hounsfield units in a region of interest as a proxy for image quality is also a limitation of this study. The effect of the combined use of bismuth shields and automatic tube current modulation on diagnostic quality of images needs to be assessed. Finally, our conversion factor used to compute effective dose was an estimate of a chest CT protocol for a 5-year-old because standards are not available for pediatric chest 16-MDCT. Although the effective dose would differ if another conversion factor were used, the change in the effective dose we determined (13% decrease) when the shield was placed after the scout compared with when the shield was present in the scout is independent of the factor used.

In conclusion, the use of a bismuth breast shield in addition to one technique for z-axis automatic tube current modulation further reduces detected radiation dose as determined in a pediatric anthropomorphic phantom. Dose reduction is greatest when the breast shield is placed after the scout radiograph is obtained. Although placing the breast shield after the scout radiograph is obtained does result in increased image noise in the range of the shield because the tube current is calculated without factoring in the attenuation of the breast shield, the increased image noise is still close to the noise target level.

References

1. Linton OW, Mettler FA Jr. National conference on dose reduction in CT, with an emphasis on pediatric patients. *AJR* 2003; 181:321–329
2. Frush DP, Applegate K. Computed tomography and radiation: understanding the issues. *J Am Coll Radiol* 2004; 1:113–119
3. Brenner DJ, Elliston CD, Hall EJ, Berdon WE. Estimated risks of radiation-induced fatal cancer from pediatric CT. *AJR* 2001; 176:289–296

Pediatric Chest MDCT with Tube Current Modulation

4. Karlsson P, Holmberg E, Lundell M, Mattsson A, Holm LE, Wallgren A. Intracranial tumors after exposure to ionizing radiation during infancy: a pooled analysis of two Swedish cohorts of 28,008 infants with skin hemangioma. *Radiat Res* 1995; 150:357–364
5. Tack D, De Maertelaer V, Gevenois PA. Dose reduction in multidetector CT using attenuation-based online tube current modulation. *AJR* 2003; 181:331–334
6. Greess H, Lutze J, Nömayr A, et al. Dose reduction in subsecond multislice spiral CT examination of children by online tube current modulation. *Eur Radiol* 2004; 14:995–999
7. Kalra MK, Rizzo S, Maher M, et al. Chest CT performed with z-axis modulation: scanning protocol and radiation dose. *Radiology* 2005; 237:303–308
8. Kalra MK, Maher MM, Toth TL, Kamath RS, Halpern EF, Saini S. Comparison of z-axis automatic tube current modulation technique with fixed tube current CT scanning of abdomen and pelvis. *Radiology* 2004; 232:347–353
9. Kalra MK, Maher MM, Kamath RS, et al. Sixteen-detector row CT of abdomen and pelvis: study for optimization of z-axis modulation technique performed in 153 patients. *Radiology* 2004; 233:241–249
10. Mulkens TH, Bellinck P, Baevaert M, et al. Use of an automatic exposure control mechanism for dose optimization in multi-detector row CT examinations: clinical evaluation. *Radiology* 2005; 237:213–223
11. Kalendar WA, Wolf H, Suess C, Gies M, Greess H, Bautz WA. Dose reduction in CT by on-line tube current control: principles and validation on phantoms and cadavers. *Eur Radiol* 1999; 9:323–328
12. Mastora I, Remy-Jardin M, Suess C, Scherf C, Guillot JP, Remy J. Dose reduction in spiral CT angiography of thoracic outlet syndrome by anatomically adapted tube current modulation. *Eur Radiol* 2001; 11:590–596
13. Perisinakis K, Raissaki M, Tzedakis A, Theocharopoulos N, Damilakis J, Gourtsoyiannis N. Reduction of eye lens radiation dose by orbital bismuth shielding in pediatric patients undergoing CT of the head: a Monte Carlo study. *Med Phys* 2005; 32:1024–1030
14. Fricke BL, Donnelly LF, Frush DP, et al. In-plane bismuth breast shields for pediatric CT: effects on radiation dose and image quality using experimental and clinical data. *AJR* 2003; 180:407–411
15. Hopper KD, King SH, Lobell ME, TenHave TR, Weaver JS. The breast: in-plane x-ray protection during diagnostic thoracic CT—shielding with bismuth radioprotective garments. *Radiology* 1997; 205:853–858
16. Kalra MK, Maher MM, Toth TL, et al. Techniques and applications of automatic tube current modulation for CT. *Radiology* 2004; 233:649–657
17. *Atom pediatric 5-year-old phantom user manual: model 705-D handling instructions*. Norfolk, VA: CIRS, 2002
18. Peet DJ, Pryor MD. Evaluation of a MOSFET radiation sensor for the measurement of entrance surface dose in diagnostic radiology. *BJR* 1999; 72:562–568
19. Yoshizumi T, Goodman P, Frush DP, et al. Validation of metal oxide semiconductor field effect transistor technology for organ dose assessment during CT: comparison with thermoluminescent dosimetry. *AJR* 2007; 188:1332–1336
20. Hurwitz LM, Yoshizumi TT, Goodman P, et al. Effective dose determination using an anthropomorphic phantom and metal oxide semiconductor field effect transistor technology for clinical adult body multidetector array computed tomography protocols. *J Comput Assist Tomogr* 2007 31:544–549
21. Shrimpton PC, Wall BF. Reference doses for paediatric computed tomography. *Radiat Prot Dosim* 2000; 90:249–252
22. Hollingsworth CL, Frush DP, Yoshizumi TT, et al. Pediatric cardiac-gated CT angiography: assessment of radiation dose. *AJR* 2007; 189:12–18
23. Travis LB, Hill D, Dores GM, et al. Cumulative absolute breast cancer risk for young women treated for Hodgkin lymphoma. *J Natl Cancer Inst* 2005; 97:1428–1437
24. Land CE, Tokunaga M, Koyama K, et al. Incidence of female breast cancer among atomic bomb survivors, Hiroshima and Nagasaki, 1950–1990. *Radiat Res* 2003; 160:707–717
25. Miller AB, Howe GR, Sherman GJ, et al. Mortality from breast cancer after irradiation during fluoroscopic examinations in patients being treated for tuberculosis. *N Engl J Med* 1989; 321:1285–1289
26. Hildreth NG, Shore RE, Dvoretzky PM. The risk of breast cancer after irradiation of the thymus in infancy. *N Engl J Med* 1989; 321:1281–1284
27. Frush DP. Pediatric CT: practical approach to diminish the radiation dose. *Pediatr Radiol* 2002; 32:714–717
28. McCollough CH, Bruesewitz MR, Kofler JM Jr. CT dose reduction and dose management tools: overview of available options. *RadioGraphics* 2006; 26:503–512
29. Hurwitz LM, Yoshizumi TT, Reiman RE, et al. Radiation dose to the female breast from 16-MDCT body protocols. *AJR* 2006; 186:1718–1722